Stony Brook University

Brookhaven National Laboratory

UCLA Mani L. Bhaumik Institute for Theoretical Physics

Dijets at small-x beyond TMDs

CFNS Workshop:
Jets for 3D imaging at the EIC
September 29th, 2021

Center for Frontiers in Nuclear Science

Farid Salazar

SBU/BNL ⟶ UCLA

Outline

- Dijet production in the TMD formalism

- Dijet production beyond TMDs: CGC formalism

- Dijet production in the CGC at NLO

- Summary and Outlook

Dijet and dihadron production: TMD formalism

Quark initiated vs gluon initiated channels

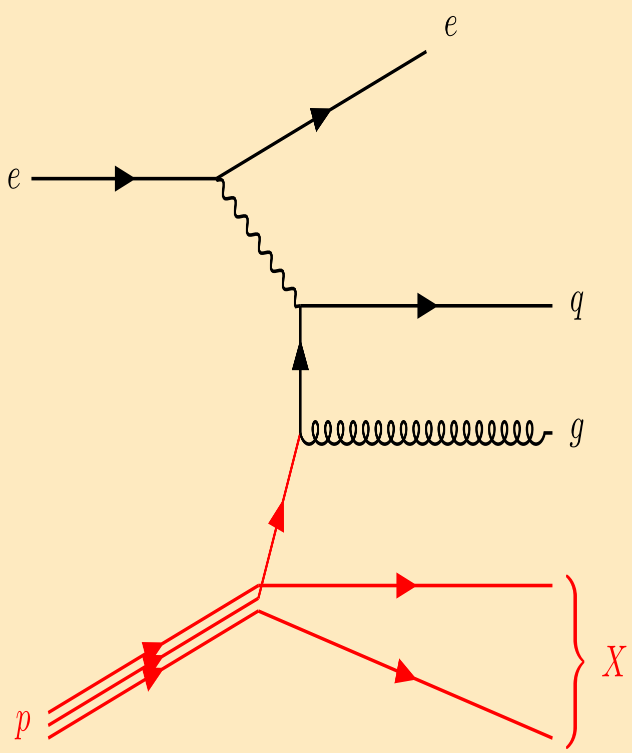

QCD Compton scattering

~ quark PDF

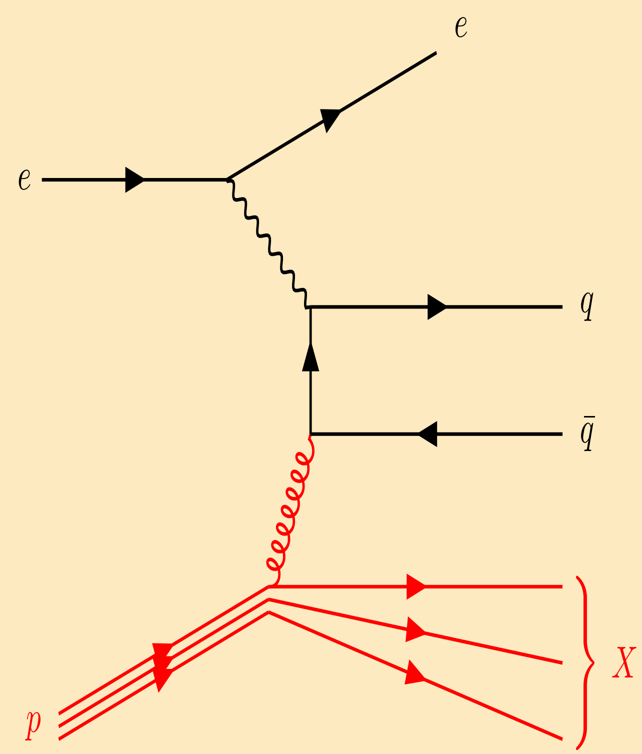

Photon-gluon fusion

~ gluon PDF

dominant channel at small-x

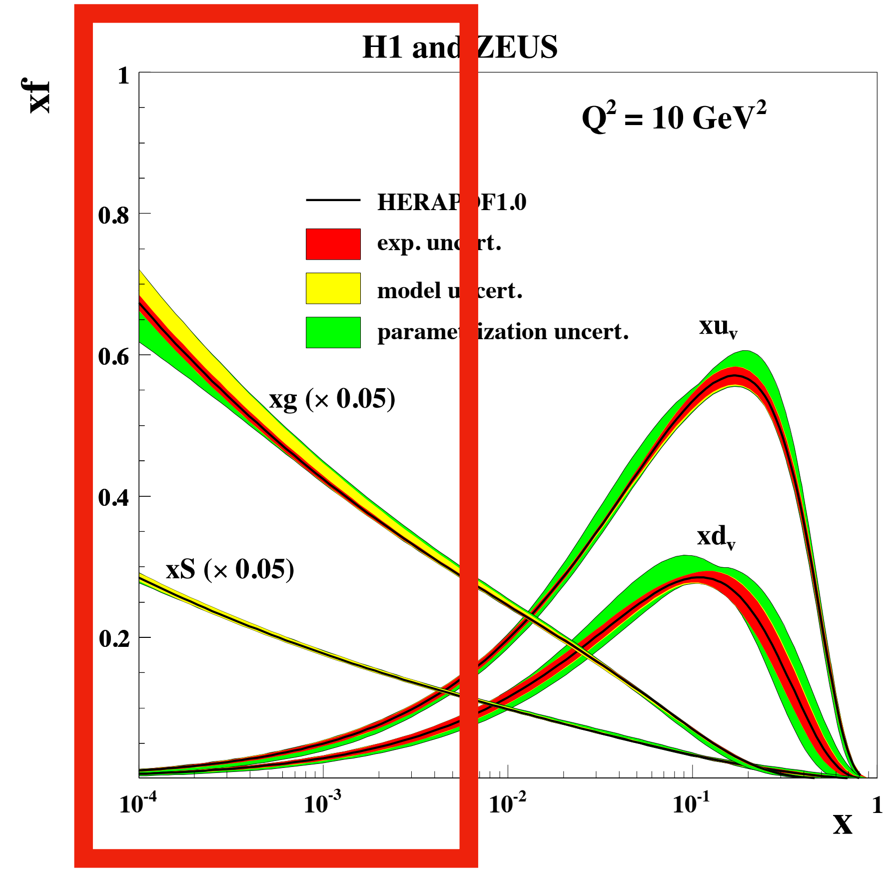

Image source: H1Zeus

Dijet and dihadron production: TMD formalism

The Weizsäcker-Williams gluon TMD

Bomhof, Mulders, Pijlman (2006)
Dominguez, Marquet, Xiao, Yuan (2011)
Dominguez, Qiu, Xiao, Yuan (2011)

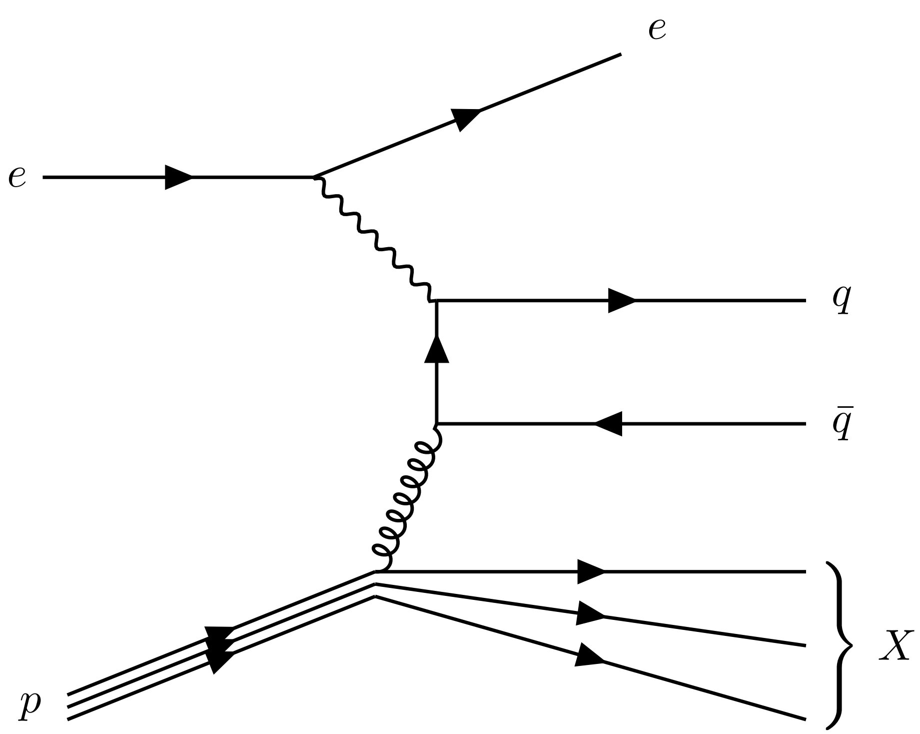

LO diagram for $q\bar{q}$ production

$$d\sigma^{\gamma^* A \to q\bar{q}X} \sim \mathcal{H}^{ij}_{\mathrm{TMD}}(\boldsymbol{P}_\perp)\, \alpha_s x G^{ij}_{\mathrm{WW}}(x, \boldsymbol{k}_\perp)$$

Perturbatively calculable — WW gluon TMD

For more on dijets and TMDs see Ignazio's talk

$$xG^{ij}_{\mathrm{WW}}(x, \boldsymbol{k}_\perp) = \frac{1}{2}\delta^{ij} xG^{0}_{\mathrm{WW}}(x, k_\perp) \quad \text{Unpolarized}$$

$$+\Pi^{ij}(\boldsymbol{k}_\perp) xh^{0}_{\mathrm{WW}}(x, k_\perp) \quad \text{Linearly polarized}$$

$$\Pi^{ij}(\boldsymbol{k}_\perp) = \left(2\frac{\boldsymbol{k}^i_\perp \boldsymbol{k}^j_\perp}{\boldsymbol{k}^2_\perp} - \delta^{ij}\right)$$

Validity of TMD approach:

$k_\perp \ll P_\perp$ (i.e. back-to-back configuration)

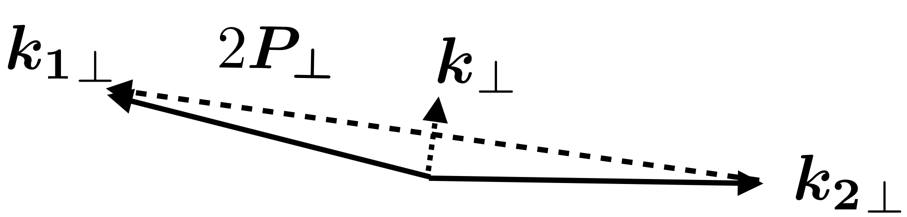

$$\boldsymbol{k}_\perp = \boldsymbol{k}_{1\perp} + \boldsymbol{k}_{2\perp}$$

$$\boldsymbol{P}_\perp = z_2 \boldsymbol{k}_{1\perp} - z_1 \boldsymbol{k}_{2\perp}$$

Dijet and dihadron production: TMD formalism

Forward dihadron azimuthal correlations and gluon saturation

Weizsäcker-Williams TMD
at small-x

→

Dihadron suppression
back-to-back peak

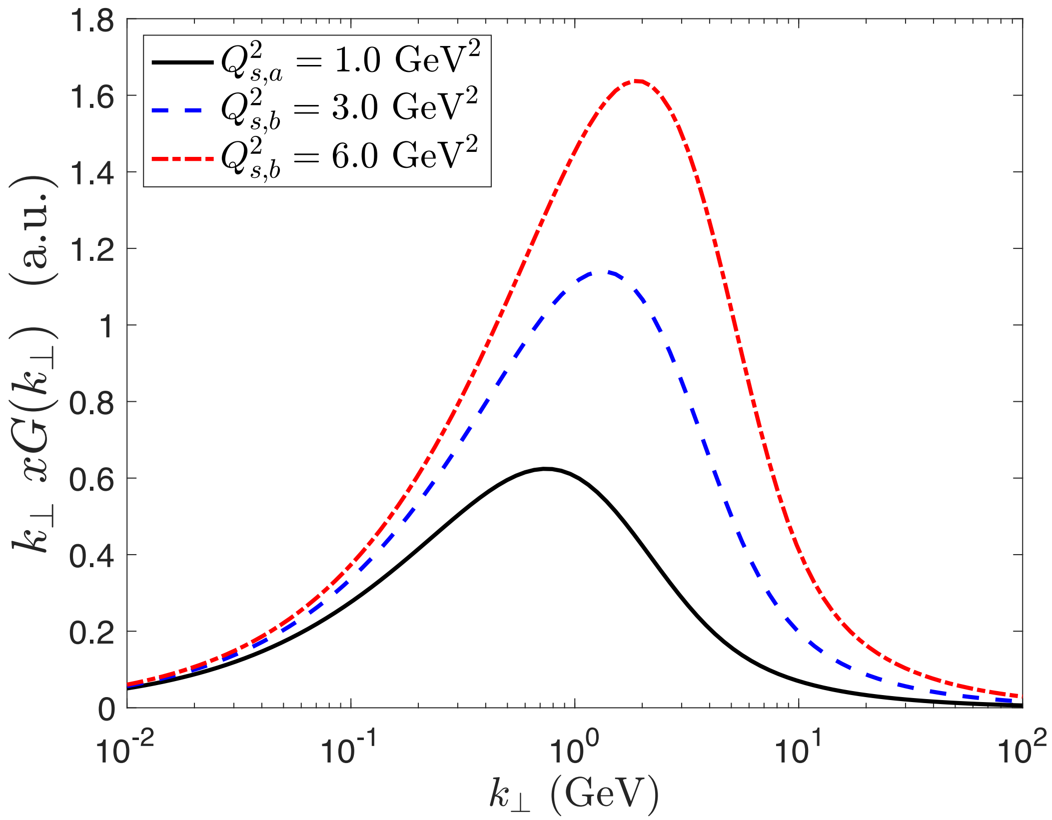

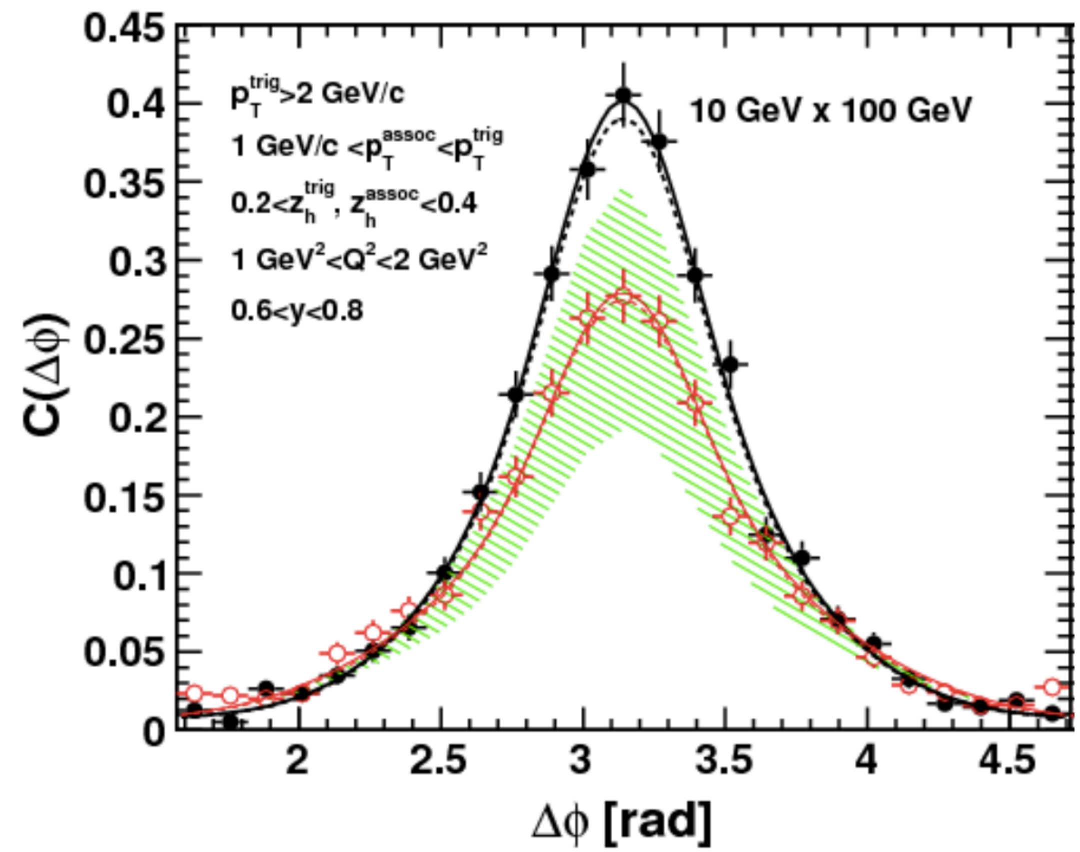

Typical momentum transfer from
hadron/nucleus to

Momentum imbalance → $k_\perp \sim Q_s$ ← Saturation scale

Zheng, Aschenauer, Lee, Xiao (2014)

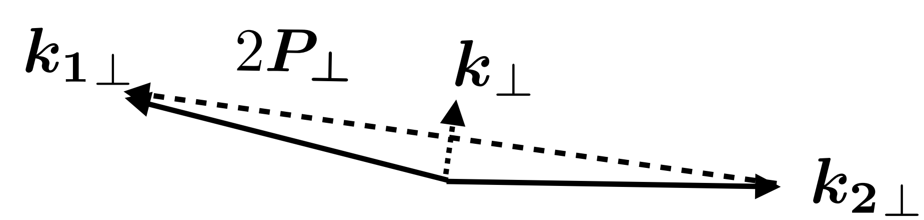

$\Delta\phi$ angle between $k_{1\perp}$ and $k_{2\perp}$

Dijet and dihadron production: TMD formalism

Forward dijet azimuthal asymmetries and WW gluon TMD

Ratio of linearly polarized to unpolarized gluon WW

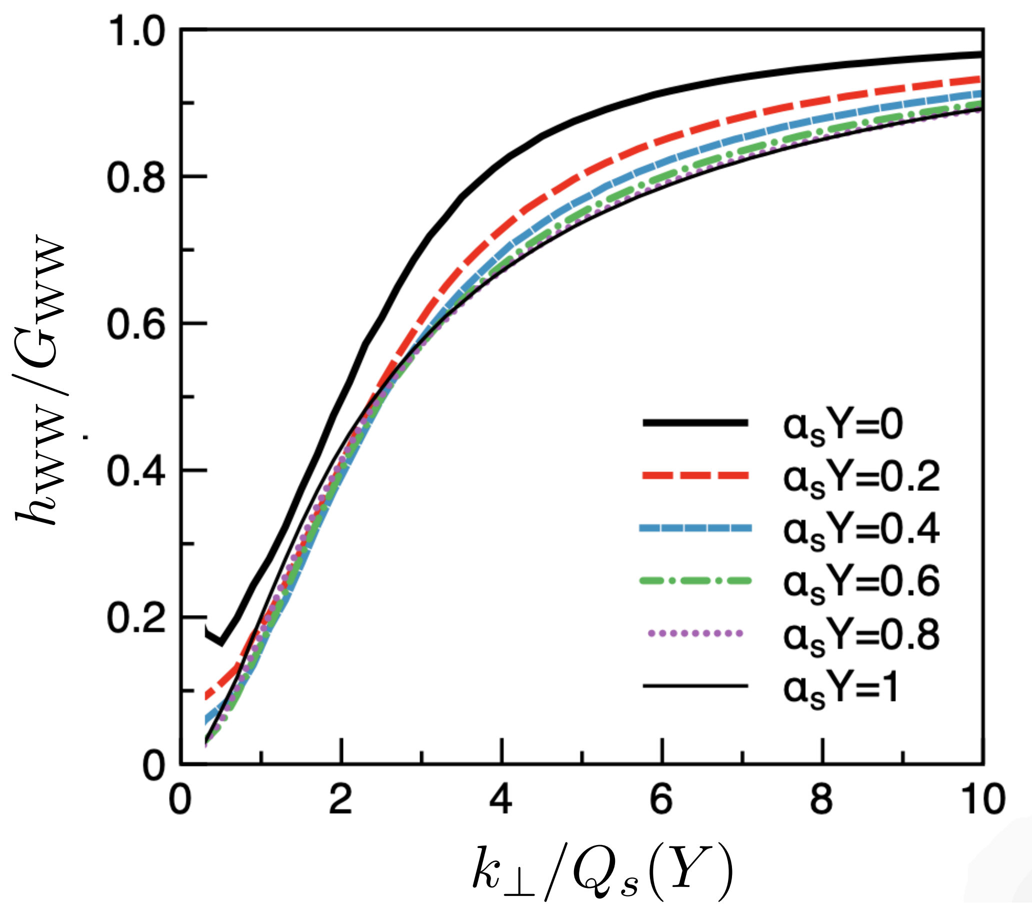

Dumitru, Lappi, Skokov (2015)

→

Dijet azimuthal asymmetries in momentum imbalance

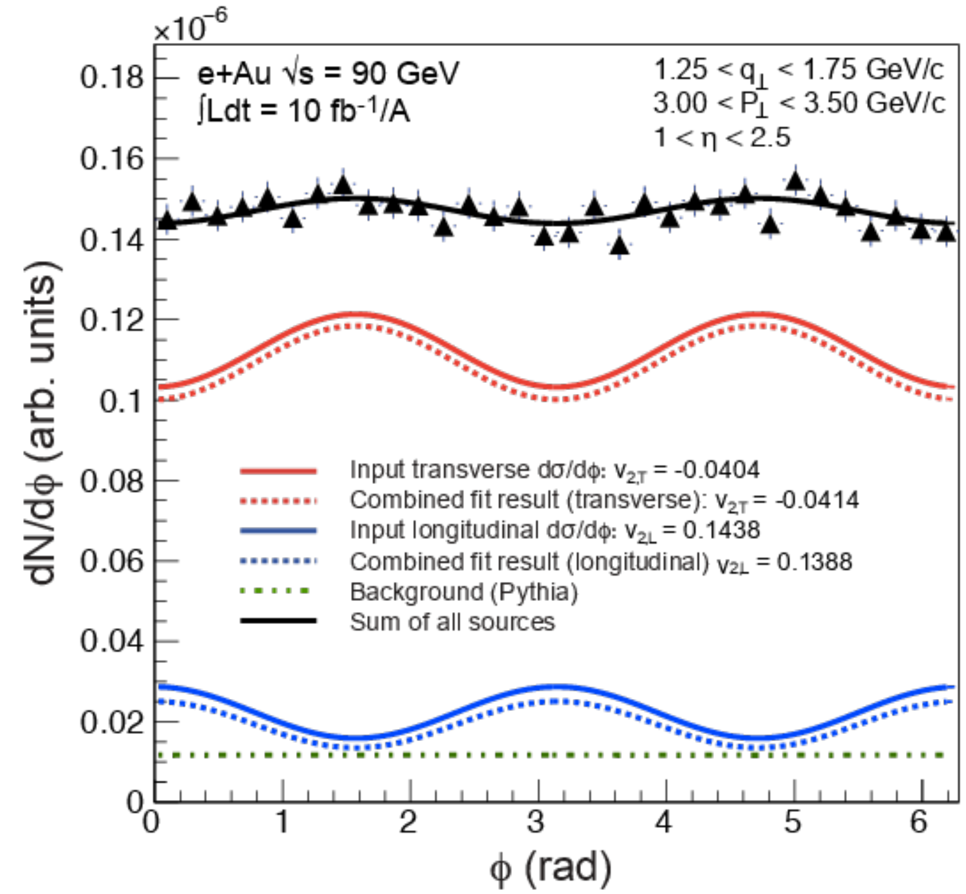

Dumitru, Skokov, Ullrich (2018)

Accessed in azimuthal asymmetry of momentum imbalance in dijet pairs

Dominguez, Qiu, Xiao, Yuan (2011)

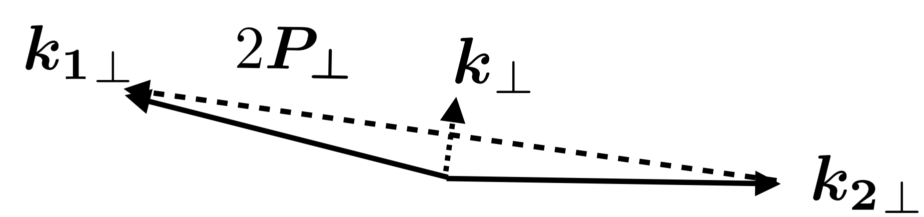

ϕ angle between $\boldsymbol{P}_\perp$ and $\boldsymbol{k}_\perp$

$$|v_2| \sim \frac{xh_{WW}}{xG_{WW}}$$

Dijet production beyond TMDs

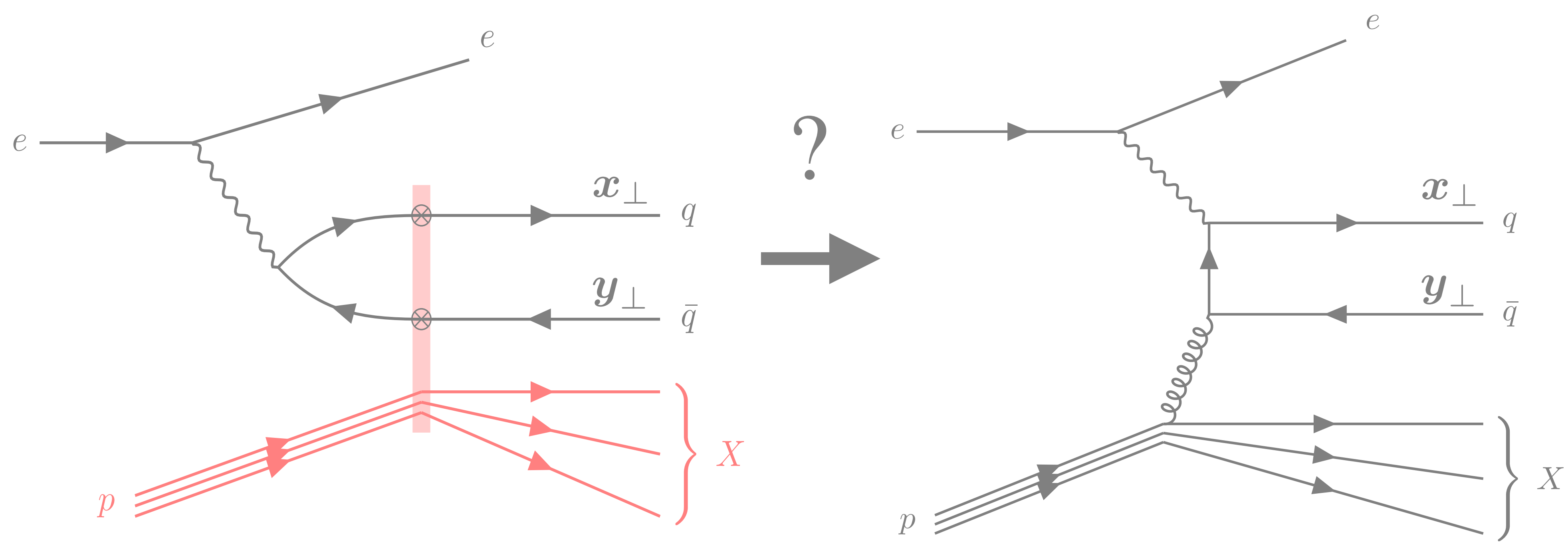

A comprehensive numerical study of the TMD/CGC correspondence

H. Mäntysaari, N. Mueller, FS, and B. Schenke. Phys.Rev.Lett. 124 (2020)
R. Boussarie, H. Mäntysaari, FS, and B. Schenke. 2106.11301 (Accepted to JHEP)

Dijet production beyond TMDs

Computation in the CGC: Wilson Lines

Dominguez, Marquet, Xiao, Yuan (2011)

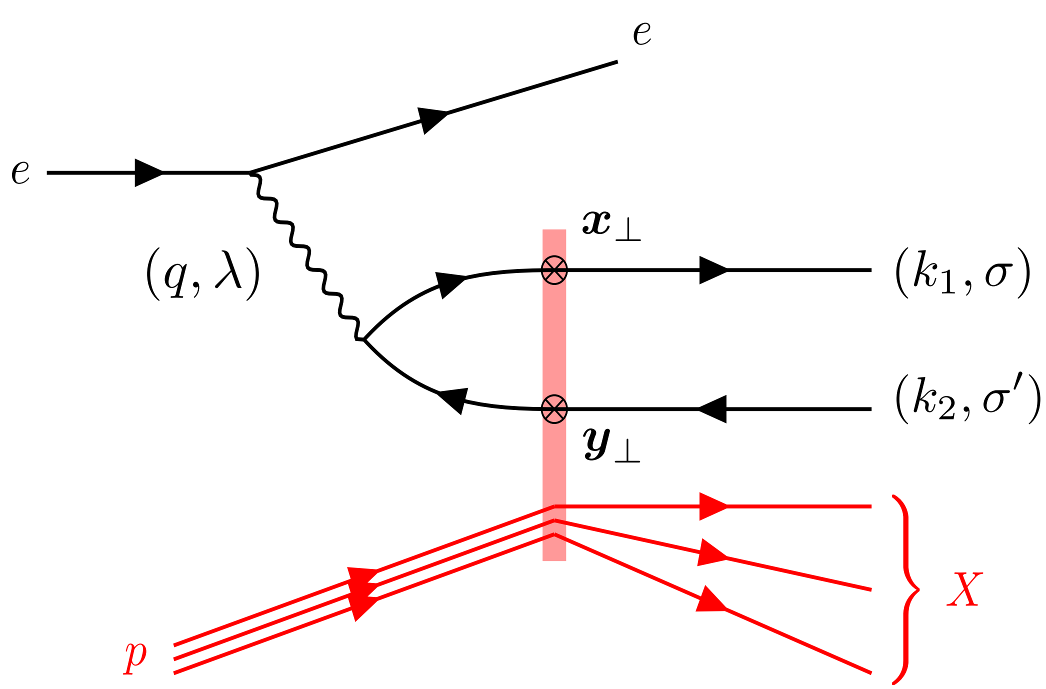

LO diagram for $q\bar{q}$ production in the CGC EFT

Dense gluon field $A_{\rm cl} \sim 1/g$ **needs resummation of multiple gluon interactions**

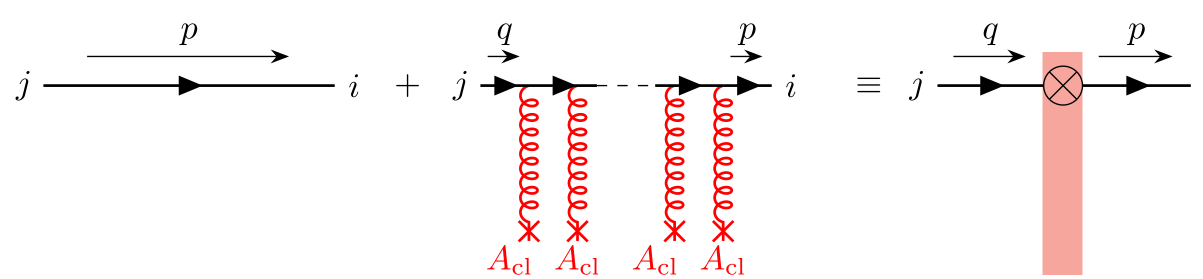

$$V_{ij}(\boldsymbol{x}) = P \exp\left\{ ig \int dx^- A^{+,a}_{cl}(\boldsymbol{x}, x^-) t^a \right\}$$

Amplitude (modulo leptonic part):

$$\mathcal{M}^{\lambda\sigma\sigma'}_{\rm LO} = \Psi^{\gamma^*_\lambda \to q\bar{q}}(Q, \mathbf{r}_{xy}, z_q) \otimes_{\rm LO} \left[1 - V(\boldsymbol{x}_\perp) V^\dagger(\boldsymbol{y}_\perp)\right]$$

perturbatively computable — non-perturbative

$$\otimes_{\rm LO} \equiv \frac{e e_f q^-}{\pi} \int \mathrm{d}^2\boldsymbol{x}_\perp \mathrm{d}^2\boldsymbol{y}_\perp e^{-i\boldsymbol{k_1}_\perp\cdot\boldsymbol{x}_\perp} e^{-i\boldsymbol{k_2}_\perp\cdot\boldsymbol{y}_\perp}$$

Dijet cross-section in the CGC will contain dipoles and quadrupole:

$$\frac{1}{N_c}\left\langle \mathrm{Tr}\left[V(\boldsymbol{x}_\perp) V^\dagger(\boldsymbol{y}_\perp)\right]\right\rangle_Y$$

$$\frac{1}{N_c}\left\langle \mathrm{Tr}\left[V(\boldsymbol{x}_\perp) V^\dagger(\boldsymbol{y}_\perp) V(\boldsymbol{y}'_\perp) V^\dagger(\boldsymbol{x}'_\perp)\right]\right\rangle_Y$$

Dijet production beyond TMDs

CGC, improved TMD and TMD frameworks

Boussarie, Mehtar-Tani (2020)

Pair of Wilson lines as transverse gauge link

Covariant gauge

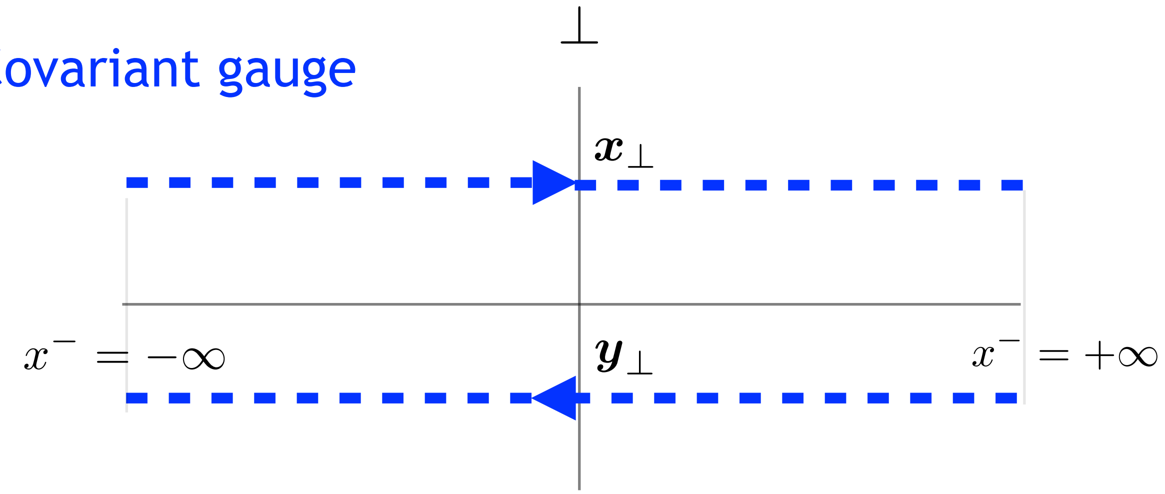

Light-cone gauge $\tilde{A}^+ = 0$

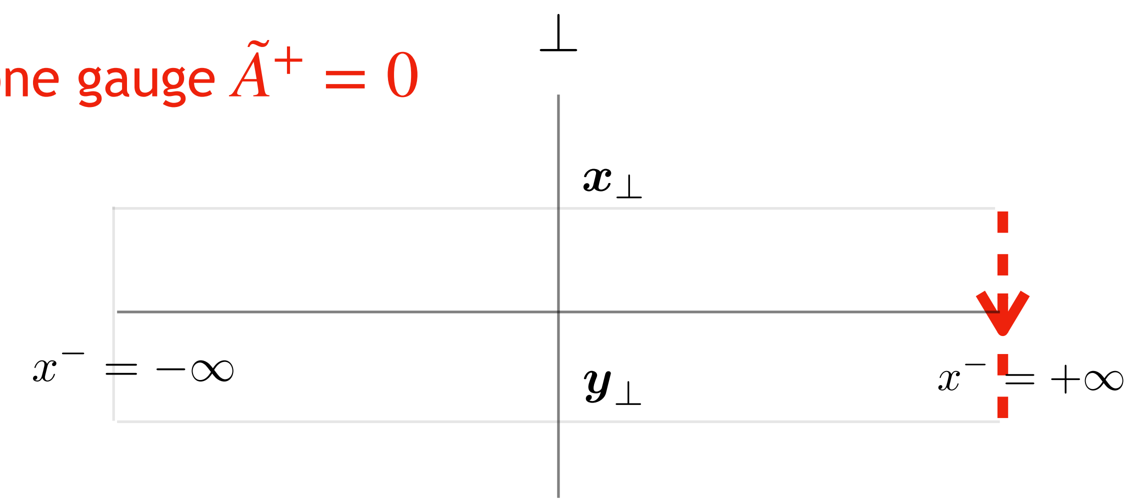

$$V(\boldsymbol{x}_\perp)V^\dagger(\boldsymbol{y}_\perp) = \mathcal{P}\exp\left[-ig\int_{\boldsymbol{y}_\perp}^{\boldsymbol{x}_\perp} \mathrm{d}\boldsymbol{z}_\perp \cdot \tilde{\boldsymbol{A}}_\perp(\boldsymbol{z}_\perp)\right]$$

gA expansion:

$$= 1 - ig\int_{\boldsymbol{y}_\perp}^{\boldsymbol{x}_\perp} \mathrm{d}\boldsymbol{z}_\perp \cdot \tilde{\boldsymbol{A}}_\perp(\boldsymbol{z}_\perp) + \ldots$$

Small dipole expansion:

Altinoluk, Boussarie, Kotko (2019)

$$= 1 + ig\,\boldsymbol{r}_\perp \cdot \tilde{\boldsymbol{A}}_\perp(\boldsymbol{z}_\perp) + \ldots$$

$\boldsymbol{r}_\perp = \boldsymbol{x}_\perp - \boldsymbol{y}_\perp$

Dominguez, Marquet, Xiao, Yuan (2011)

Dijet production beyond TMDs

CGC, improved TMD and TMD frameworks

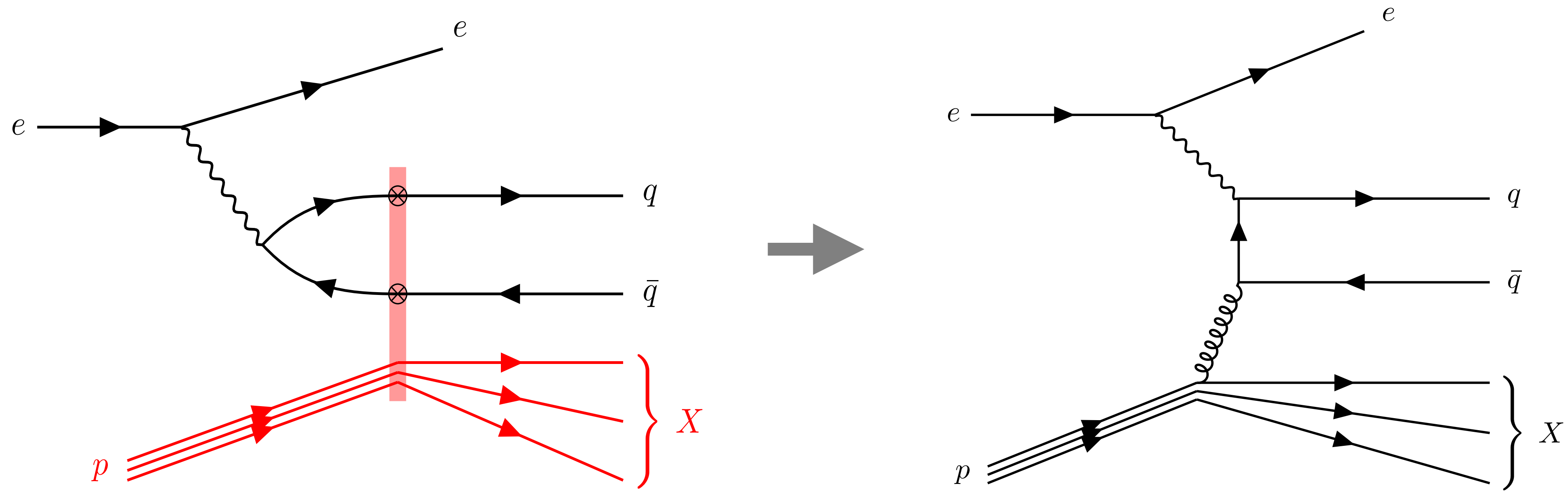

CGC

$$V(\boldsymbol{x}_\perp)V^\dagger(\boldsymbol{y}_\perp) = \mathcal{P}\,\exp\left[-ig\int_{\boldsymbol{y}_\perp}^{\boldsymbol{x}_\perp} \mathrm{d}\boldsymbol{z}_\perp \cdot \tilde{\boldsymbol{A}}_\perp(\boldsymbol{z}_\perp)\right]$$

Improved TMD

$$= 1 - ig\int_{\boldsymbol{y}_\perp}^{\boldsymbol{x}_\perp} \mathrm{d}\boldsymbol{z}_\perp \cdot \tilde{\boldsymbol{A}}_\perp(\boldsymbol{z}_\perp) + \ldots$$

TMD

Altinoluk, Boussarie, Kotko (2019)

$$= 1 + ig\ \boldsymbol{r}_\perp \cdot \tilde{\boldsymbol{A}}_\perp(\boldsymbol{z}_\perp) + \ldots$$

$\boldsymbol{r}_\perp = \boldsymbol{x}_\perp - \boldsymbol{y}_\perp$

Dominguez, Marquet, Xiao, Yuan (2011)

Dijet production beyond TMDs

The TMD and improved TMD limit as an expansion

$$\mathrm{d}\sigma_{\mathrm{CGC}} = \underbrace{\mathrm{d}\sigma_{\mathrm{TMD}} + \overbrace{\mathcal{O}\left(\frac{k_\perp}{Q_\perp}\right)}^{\text{kinematic}}}_{\mathrm{d}\sigma_{\mathrm{ITMD}}} + \overbrace{\mathcal{O}\left(\frac{Q_s}{Q_\perp}\right)}^{\text{genuine}}$$

Dominguez, Marquet, Xiao, Yuan (2011)

TMD valid $k_\perp, Q_s \ll Q_\perp$

back-to-back hadrons/jets and transverse momenta larger than sat scale

Hard factor

Weizsäcker-Williams gluon TMD

$$d\sigma^{\gamma^* A \to q\bar{q}X} \sim \mathcal{H}^{ij}_{\mathrm{TMD}}(\boldsymbol{P}_\perp)\, \alpha_s x G^{ij}_{\mathrm{WW}}(x, \boldsymbol{k}_\perp)$$

$$+\mathcal{O}(k_\perp/P_\perp) + \mathcal{O}(Q_s/P_\perp)$$

Altinoluk, Boussarie, Kotko (2019)

Improved TMD valid $Q_s \ll Q_\perp$

transverse momenta larger than sat scale

Hard factor resums kinematic powers $k_\perp/P_\perp$

$$d\sigma^{\gamma^*_\lambda A \to q\bar{q}X} \sim \mathcal{H}^{\lambda,ij}_{\mathrm{ITMD}}(\boldsymbol{P}_\perp, \boldsymbol{k}_\perp)\, \alpha_s x G^{ij}_{\mathrm{WW}}(x, \boldsymbol{k}_\perp)$$

$$+\mathcal{O}(Q_s/P_\perp)$$

Dijet production beyond TMDs

Differential yield: TMD, ITMD and CGC

R. Boussarie, H. Mäntysaari, FS, B. Schenke (2021)

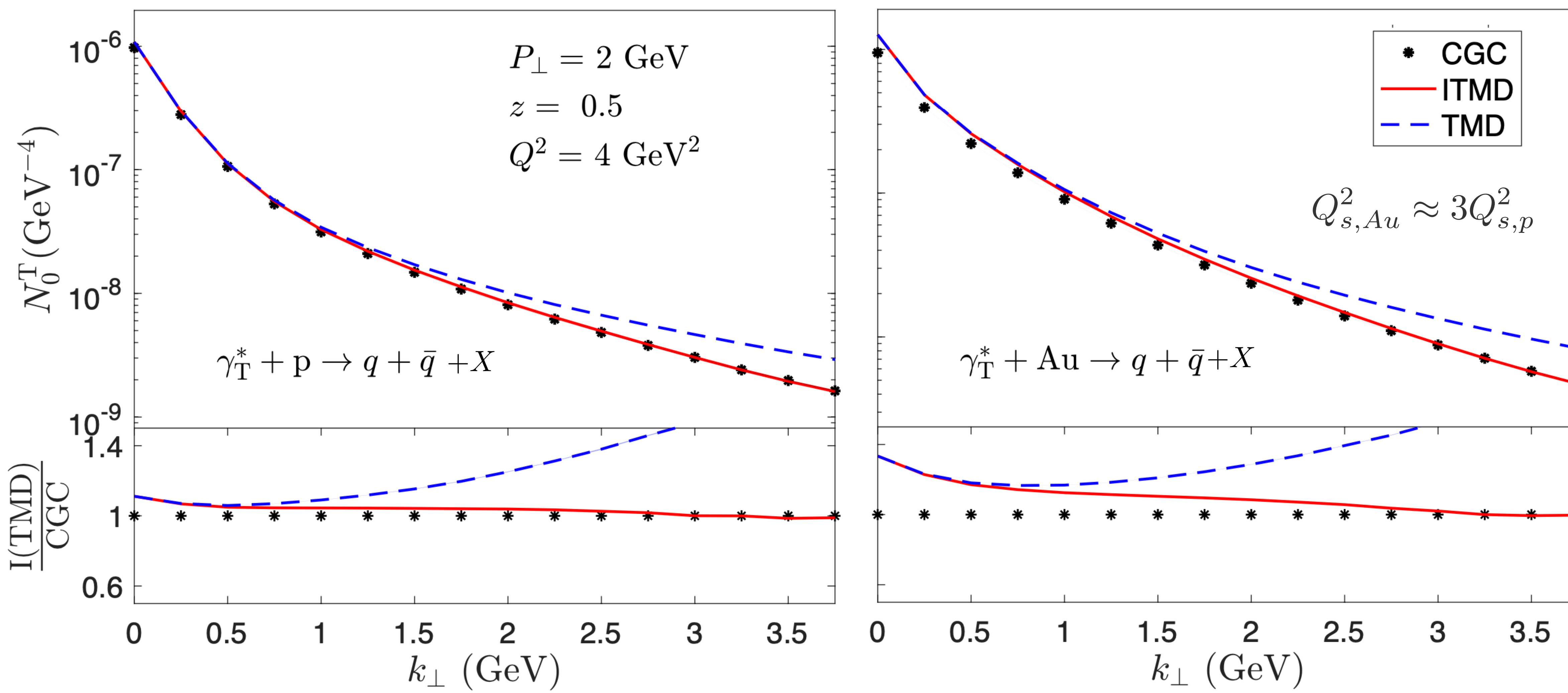

proton ~ smaller Q_s^2 **Gold nucleus** ~ **larger** Q_s^2

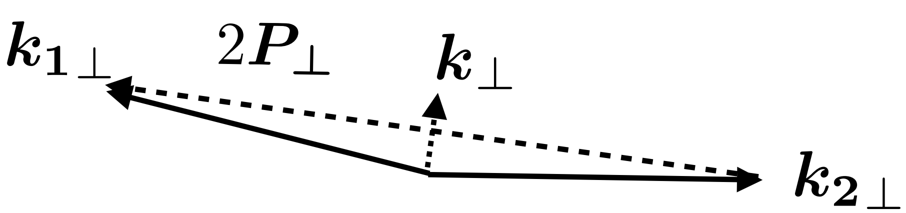

$$\frac{\mathrm{d}N^{\gamma_\lambda^*+A\to q\bar{q}+X}}{\mathrm{d}^2\boldsymbol{P}_\perp \mathrm{d}^2\boldsymbol{k}_\perp \mathrm{d}\eta_1 \mathrm{d}\eta_2} = N_0^\lambda(P_\perp, k_\perp)\left[1 + 2\sum_{k=1}^{\infty} v_{k,\lambda}(P_\perp, k_\perp)\cos(k\phi)\right]$$

$$\phi \equiv \phi_{\boldsymbol{k}_\perp} - \phi_{\boldsymbol{P}_\perp}$$

Dijet production beyond TMDs

Q^2 and $P_\perp$ dependence of genuine saturation

R. Boussarie, H. Mäntysaari, FS, B. Schenke (2021)

At exactly back-to-back $k_\perp \approx 0$ the ratio of CGC/TMD is sensitive to genuine twists

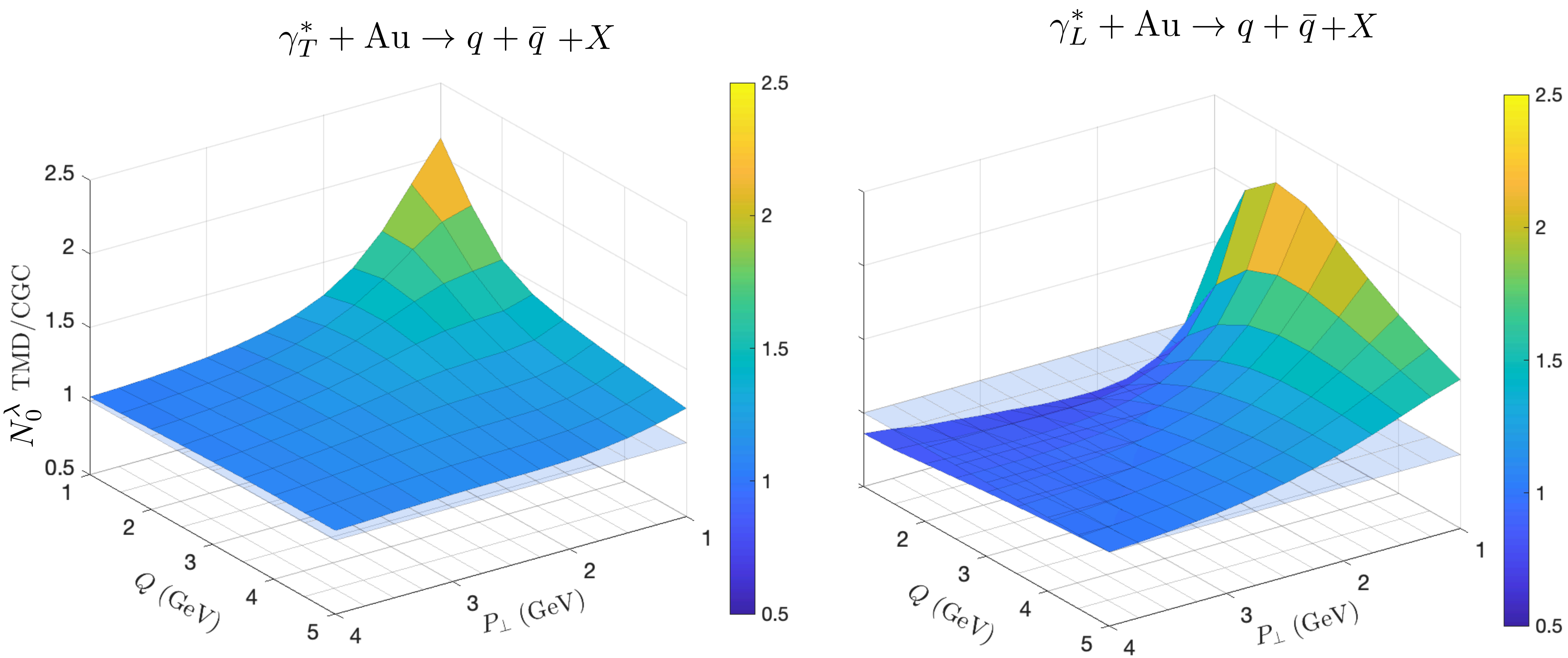

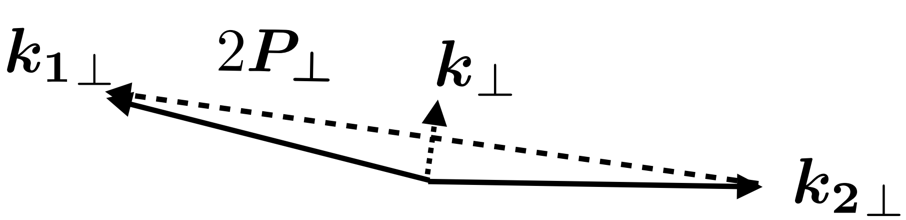

$$\frac{\mathrm{d}N^{\gamma_\lambda^*+A\to q\bar{q}+X}}{\mathrm{d}^2\boldsymbol{P}_\perp \mathrm{d}^2\boldsymbol{k}_\perp \mathrm{d}\eta_1 \mathrm{d}\eta_2} = N_0^\lambda(P_\perp, k_\perp)\left[1 + 2\sum_{k=1}^{\infty} v_{k,\lambda}(P_\perp, k_\perp)\cos(k\phi)\right]$$

$$\phi \equiv \phi_{\boldsymbol{k}_\perp} - \phi_{\boldsymbol{P}_\perp}$$

Dijet production beyond TMDs

Momentum imbalance **elliptic** anisotropies:
TMD vs ITMD

R. Boussarie, H. Mäntysaari, FS, B. Schenke (2021)

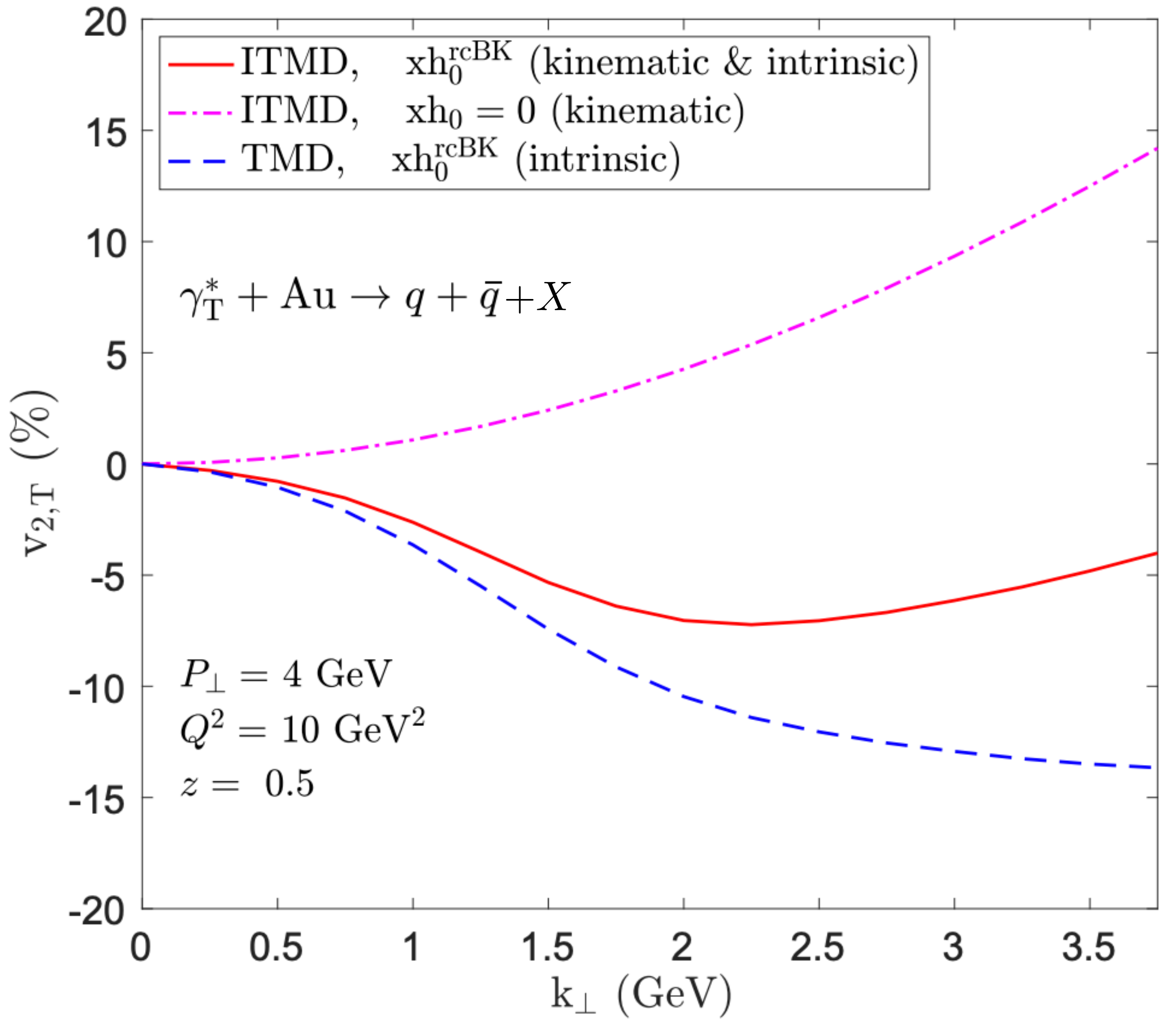

Dijet production in ITMD

Kinematic power corrections induce correlations!

$$d\sigma^{\gamma^* A \to q\bar{q}+X} \sim \mathcal{H}^G_{\rm ITMD}(\boldsymbol{P}_\perp, \boldsymbol{k}_\perp)\alpha_s x G^0_{\rm WW}(k_\perp, x)$$
$$+\mathcal{H}^h_{\rm ITMD}(\boldsymbol{P}_\perp, \boldsymbol{k}_\perp)\alpha_s x h_{\rm WW}(k_\perp, x)\cos(2\phi)$$

Elliptic anisotropy from linearly pol WW

For azimuthal correlations due to final state radiation see Feng's talk.

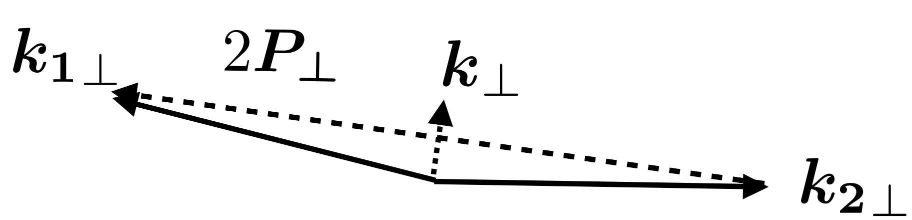

$$\frac{\mathrm{d}N^{\gamma^*_\lambda + A \to q\bar{q}+X}}{\mathrm{d}^2\boldsymbol{P}_\perp \mathrm{d}^2\boldsymbol{k}_\perp \mathrm{d}\eta_1 \mathrm{d}\eta_2} = N_0^\lambda(P_\perp, k_\perp)\left[1 + 2\sum_{k=1}^{\infty} v_{k,\lambda}(P_\perp, k_\perp)\cos(k\phi)\right]$$
$$\phi \equiv \phi_{\boldsymbol{k}_\perp} - \phi_{\boldsymbol{P}_\perp}$$

Dijet production beyond TMDs

Momentum imbalance **elliptic** anisotropies:
TMD vs ITMD vs CGC

R. Boussarie, H. Mäntysaari, FS, B. Schenke (2021)

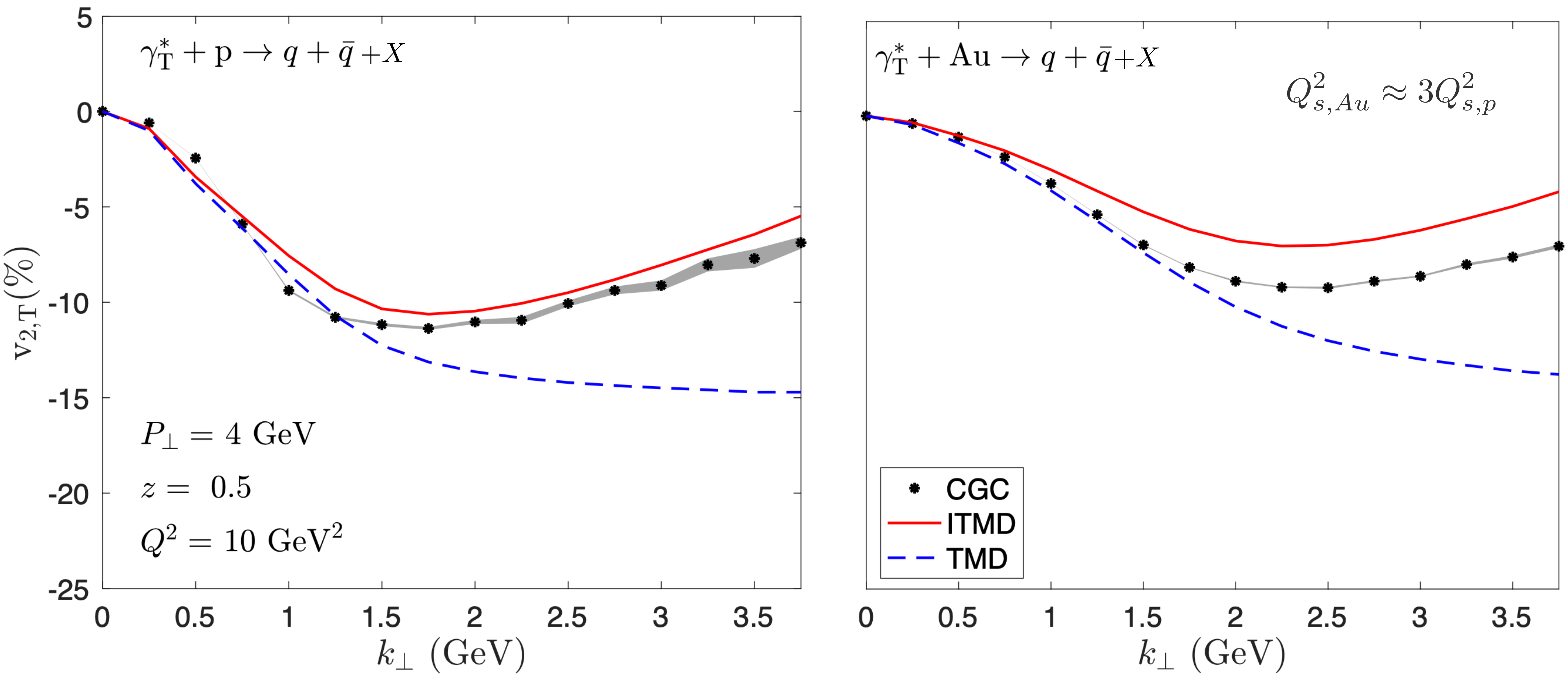

proton ~ smaller Q_s^2

Gold nucleus ~ larger Q_s^2

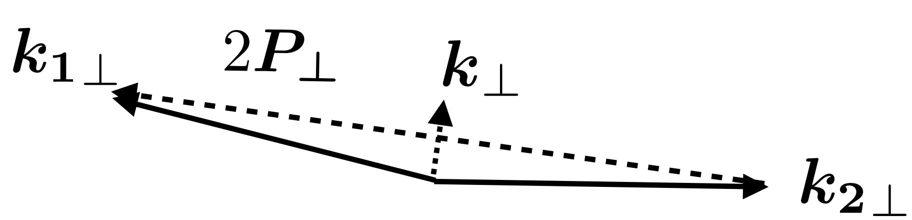

$$\frac{\mathrm{d}N^{\gamma^*_\lambda + A \to q\bar{q} + X}}{\mathrm{d}^2\boldsymbol{P}_\perp \mathrm{d}^2\boldsymbol{k}_\perp \mathrm{d}\eta_1 \mathrm{d}\eta_2} = N_0^\lambda(P_\perp, k_\perp)\left[1 + 2\sum_{k=1}^{\infty} v_{k,\lambda}(P_\perp, k_\perp)\cos(k\phi)\right]$$

$$\phi \equiv \phi_{\boldsymbol{k}_\perp} - \phi_{\boldsymbol{P}_\perp}$$

Dijet production beyond TMDs

Momentum imbalance **quadrangular** anisotropies:
TMD vs ITMD vs CGC

R. Boussarie, H. Mäntysaari, FS, B. Schenke (2021)

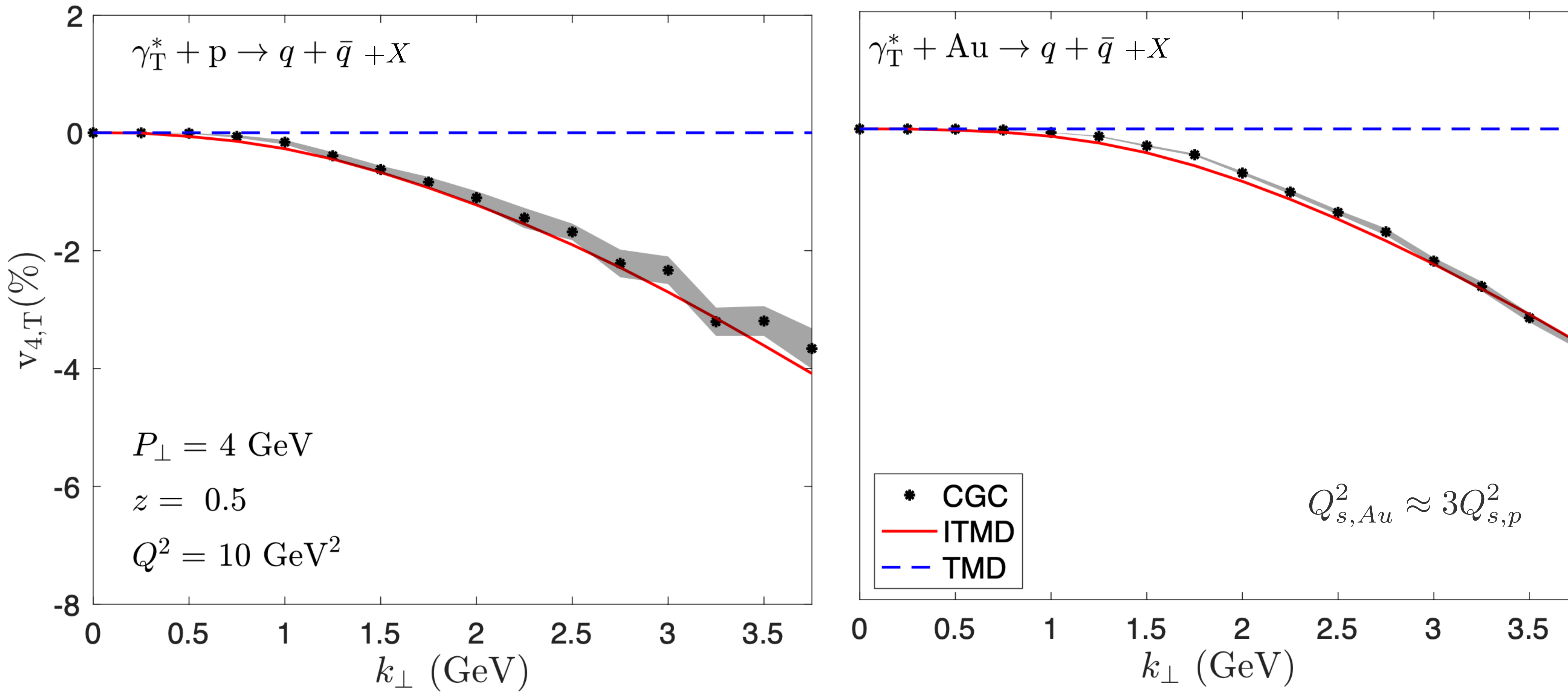

proton ~ smaller Q_s^2 **Gold nucleus ~ larger** Q_s^2

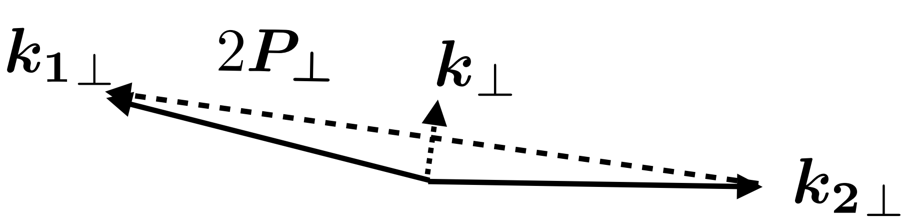

$$\frac{\mathrm{d}N^{\gamma^*_\lambda + A \to q\bar{q} + X}}{\mathrm{d}^2\boldsymbol{P}_\perp \mathrm{d}^2\boldsymbol{k}_\perp \mathrm{d}\eta_1 \mathrm{d}\eta_2} = N_0^\lambda(P_\perp, k_\perp)\left[1 + 2\sum_{k=1}^{\infty} v_{k,\lambda}(P_\perp, k_\perp)\cos(k\phi)\right]$$

$$\phi \equiv \phi_{\boldsymbol{k}_\perp} - \phi_{\boldsymbol{P}_\perp}$$

Dijet production in the CGC at NLO

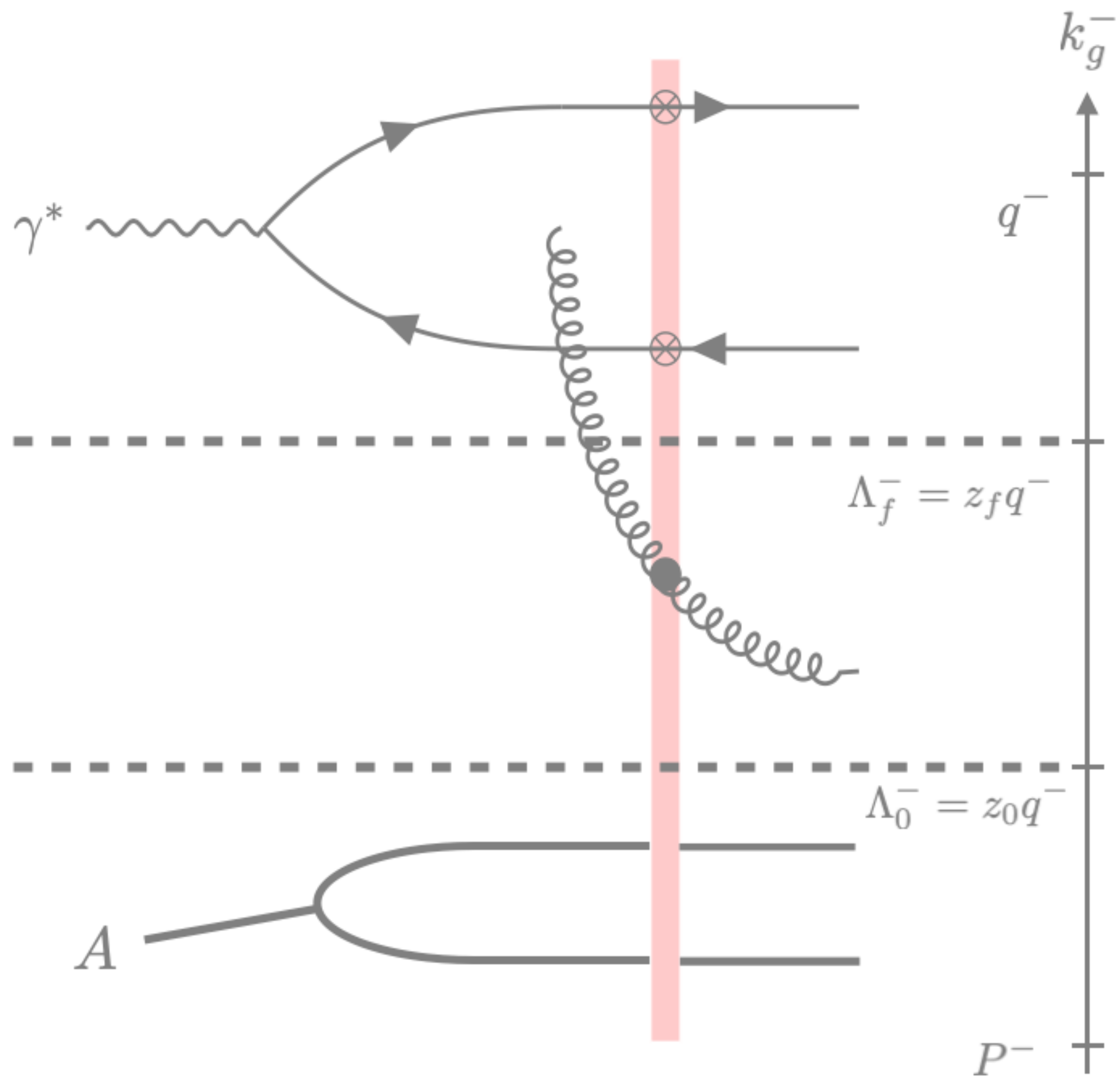

Rapidity factorization and NLO impact factor

P. Caucal, FS, and R. Venugopalan. 2108.06347

Dijet production in the CGC at NLO

Real and virtual emissions

Real emission diagrams (loop opens in DA and closes in the CCA)

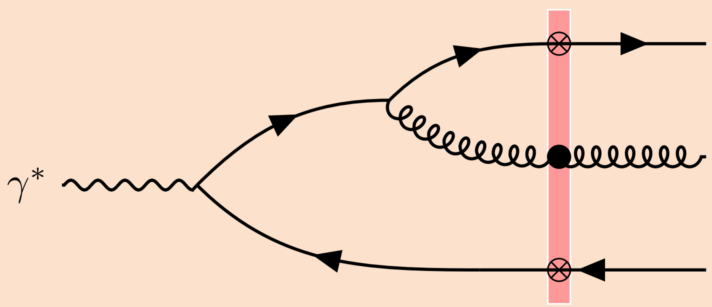

R1

$q \leftrightarrow \bar{q}$

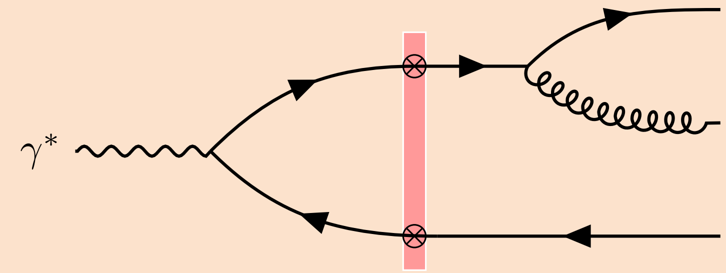

R2

$q \leftrightarrow \bar{q}$

Virtual emission (loop open and closes in DA or CCA)

Self-energy contributions

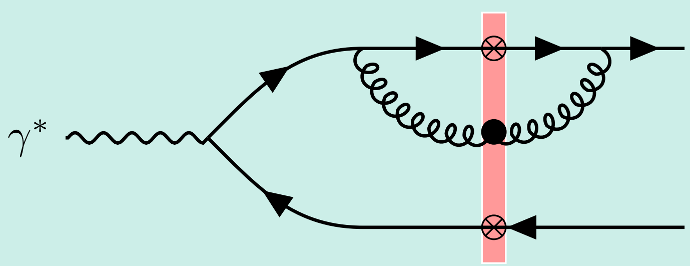

SE1

$q \leftrightarrow \bar{q}$

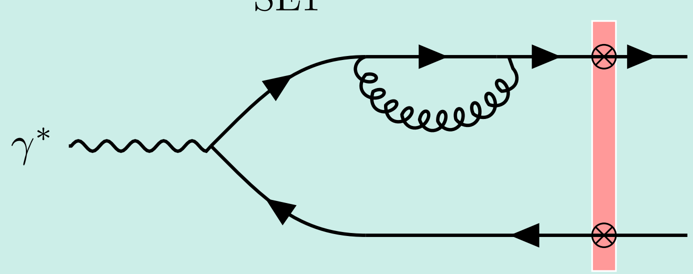

SE2

$q \leftrightarrow \bar{q}$

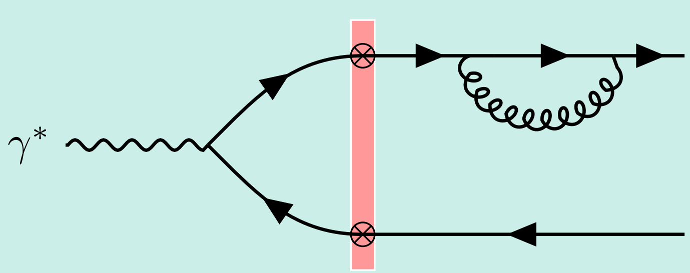

SE3

$q \leftrightarrow \bar{q}$

Vertex contributions

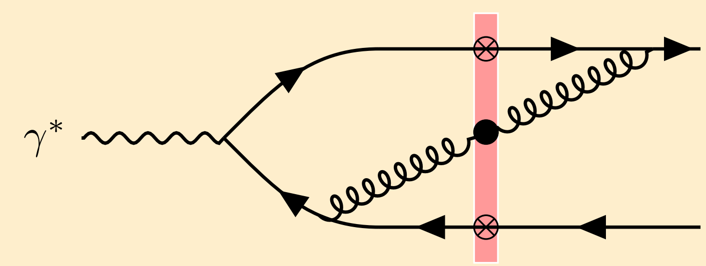

V1

$q \leftrightarrow \bar{q}$

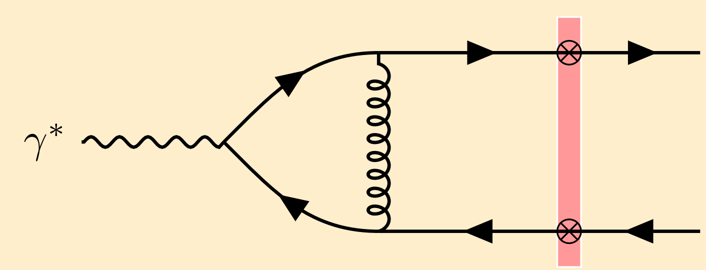

V2

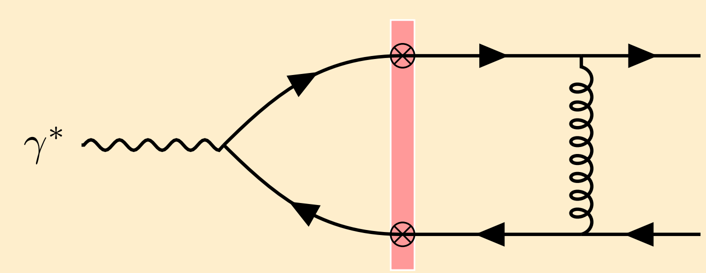

V3

Dijet production in the CGC at NLO

An example of structure of LO vs NLO amplitudes

P. Caucal, FS, and R. Venugopalan (2021)

LO amplitude

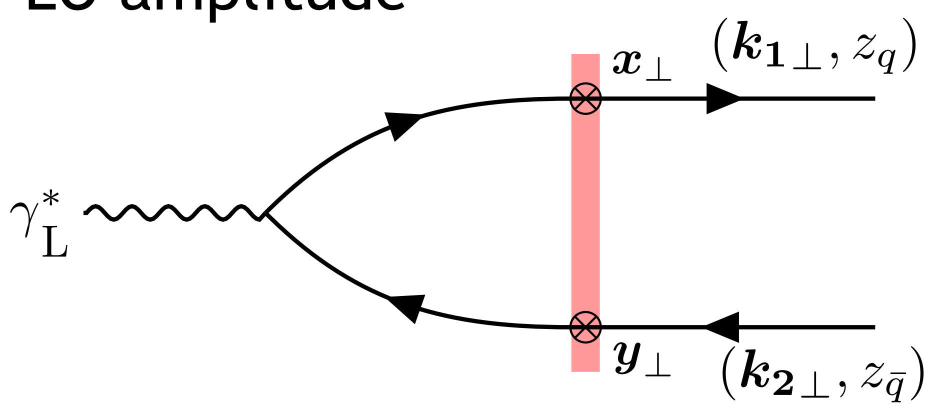

LO

$$\otimes_{\mathrm{LO}} \equiv \frac{ee_f q^-}{\pi} \int \mathrm{d}^2\boldsymbol{x}_\perp \mathrm{d}^2\boldsymbol{y}_\perp e^{-i\boldsymbol{k_1}_\perp\cdot\boldsymbol{x}_\perp} e^{-i\boldsymbol{k_2}_\perp\cdot\boldsymbol{y}_\perp}$$

$$X_{q\bar{q}}^2 = z_q z_{\bar{q}} r_{xy}^2$$ effective dipole size

$$\mathcal{M}^{\mathrm{L},\sigma\sigma'}_{\mathrm{LO}} = \left[1 - V(\boldsymbol{x}_\perp)V^\dagger(\boldsymbol{y}_\perp)\right] \otimes_{\mathrm{LO}} 2(z_q z_{\bar{q}})^{3/2} Q K_0(QX_{q\bar{q}})\delta^{\sigma,-\sigma'}$$

non-perturbative — perturbatively computable

Dressed vertex amplitude

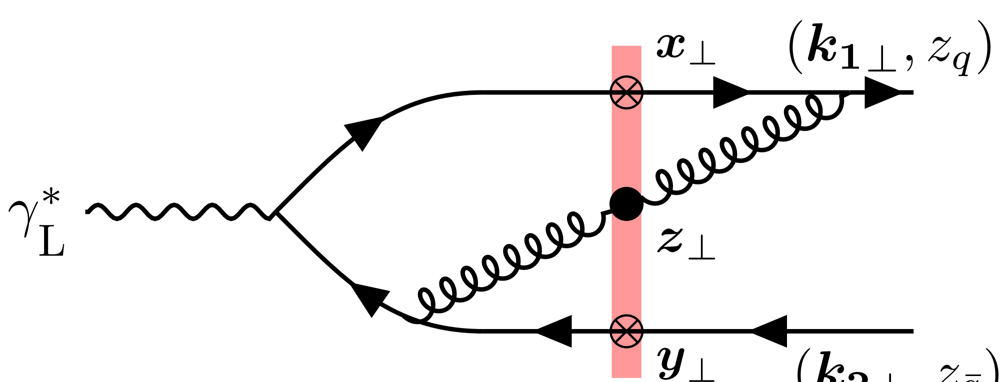

V1

$$\otimes_{\mathrm{V}} \equiv \frac{ee_f q^-}{\pi} \int \mathrm{d}^2\boldsymbol{x}_\perp \mathrm{d}^2\boldsymbol{y}_\perp \mathrm{d}^2\boldsymbol{z}_\perp e^{-i\boldsymbol{k_1}_\perp\cdot\boldsymbol{x}_\perp} e^{-i\boldsymbol{k_2}_\perp\cdot\boldsymbol{y}_\perp}$$

$$X_{q\bar{q}g}^2 = (z_q - z_g) z_{\bar{q}} r_{xy}^2 + (z_q - z_g) z_g r_{xz}^2 + z_g z_{\bar{q}} r_{zy}^2$$ effective dipole size

$$\mathcal{M}^{\mathrm{L},\sigma\sigma'}_{\mathrm{V1}} = \left[C_{\mathrm{F}}\mathbb{1} - t^a V(\boldsymbol{x}_\perp) t^b V^\dagger(\boldsymbol{y}_\perp) U_{ab}(\boldsymbol{z}_\perp)\right] \otimes_{\mathrm{V}} \frac{\alpha_s}{\pi^2} \int_{z_0}^{z_q} \frac{\mathrm{d}z_g}{z_g} \frac{\mathbf{r}_{zx}\cdot\mathbf{r}_{zy}}{\mathbf{r}_{zx}^2 \mathbf{r}_{zy}^2} \left[\left(1 - \frac{z_g}{z_q}\right)\left(1 + \frac{z_g}{z_{\bar{q}}}\right)\left(1 - \frac{z_g}{2z_q} - \frac{z_g}{2(z_{\bar{q}} + z_g)}\right) + \dots\right] e^{-i\frac{z_g}{z_q}\boldsymbol{k}_\perp\cdot\mathbf{r}_{zx}}$$

$$\times\, 2(z_q z_{\bar{q}})^{3/2} Q K_0(QX_{q\bar{q}g})\delta^{\sigma,-\sigma'}$$

non-perturbative — perturbatively computable

Dijet production in the CGC at NLO

Cancellation of divergences of UV divergences

P. Caucal, FS, and R. Venugopalan (2021)

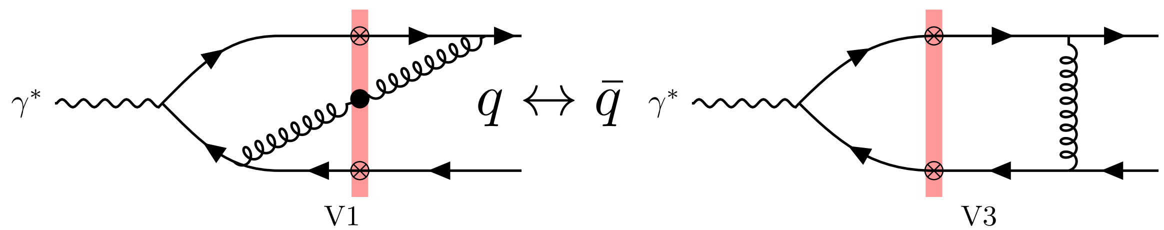

- UV finite diagrams

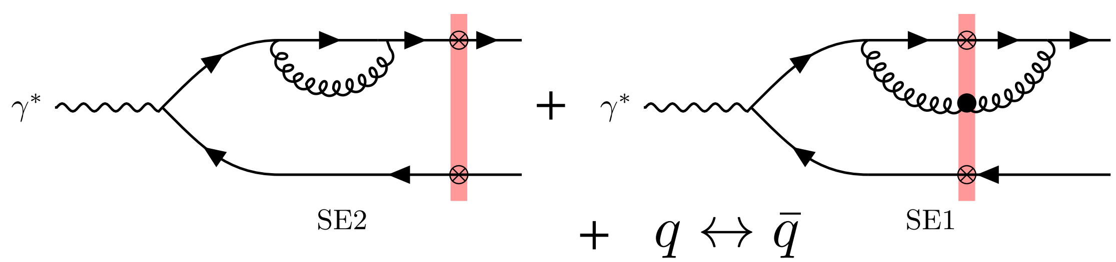

- UV divergences cancel among self energies contributions (before SW and crossing SW)

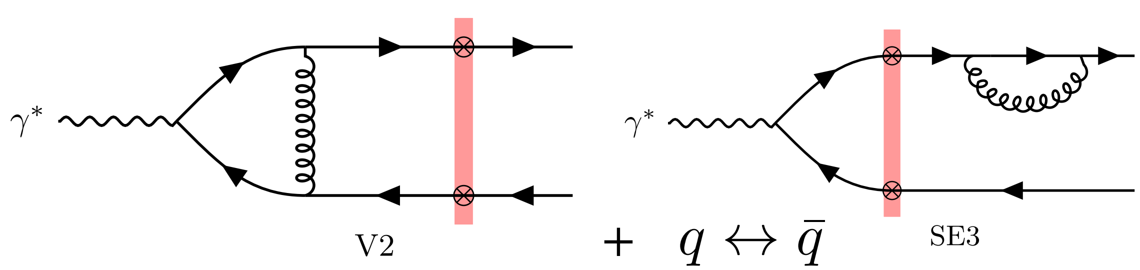

- UV divergence cancel in vertex contribution before SW and self energy contribution after SW

- <u>UV finite</u>, no need for counter-terms at this order in PT.
- Overall <u>IR divergence</u> is left in sum of virtual diagrams, and <u>soft divergence</u> left in V3. Both <u>cancel with real emissions</u>.

Inclusive dijet production at NLO

Rapidity (slow gluon) divergences and JIMWLK factorization

P. Caucal, FS, and R. Venugopalan (2021)

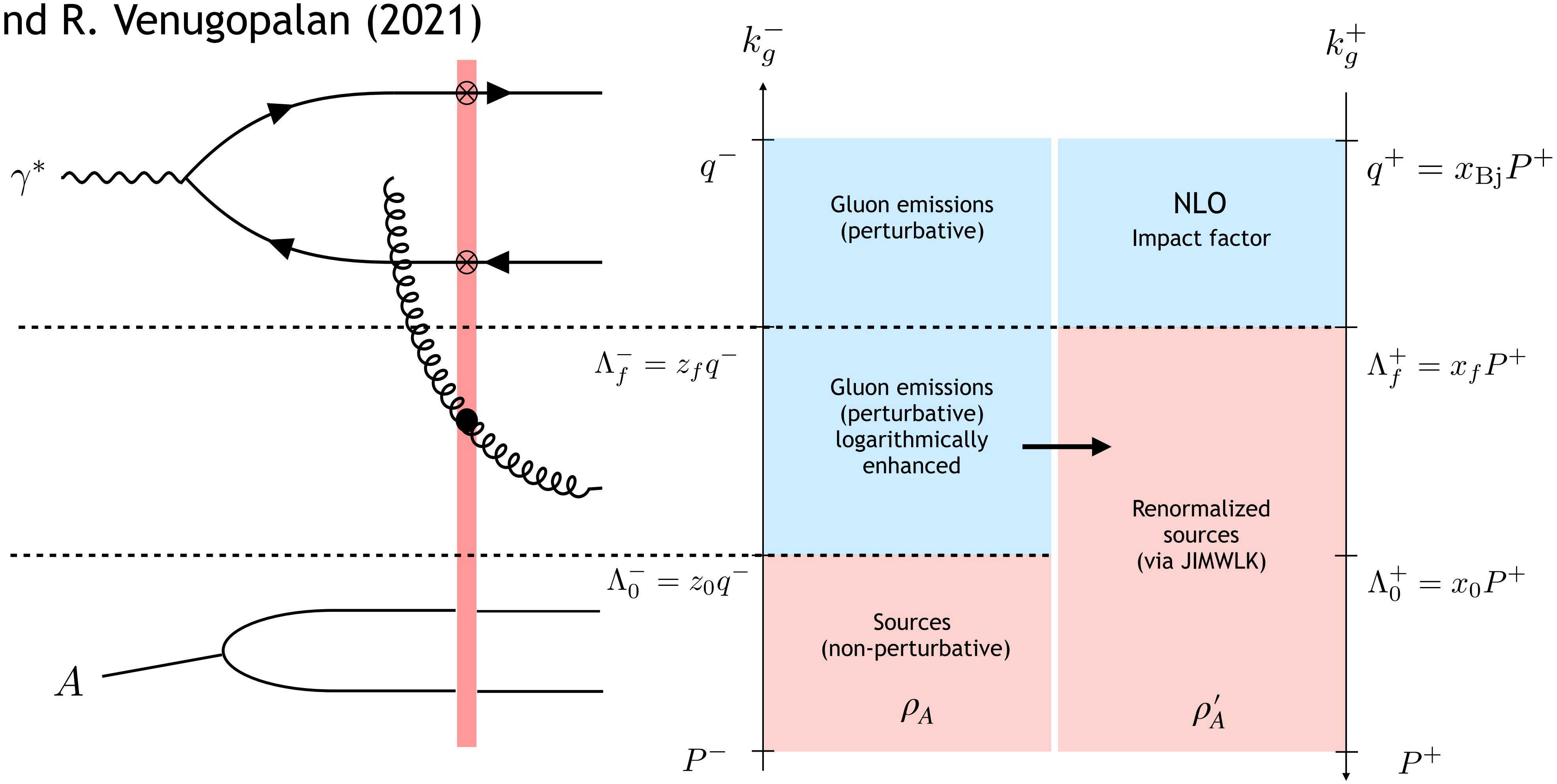

- Terms proportional to $\alpha_s \ln^2\left(\frac{z_f}{z_0}\right)$ cancel, only $\alpha_s \ln\left(\frac{z_f}{z_0}\right)$ survive and factorize:

$$\mathrm{d}\sigma_{\rm NLO} \sim \alpha_s \ln\left(\frac{z_f}{z_0}\right) \mathcal{H}_{\rm LL} \mathrm{d}\sigma_{\rm LO}$$

JIMWLK LL Hamiltonian

- Slow gluon radiation $\alpha_s \ln\left(\frac{z_f}{z_0}\right)$ can be large in resummed by redefining distribution of sources:

$$W_{x_0}[\rho_A] \to W_{x_f}[\rho'_A]$$

Dijet production in the CGC at NLO

Infrared and collinear safety

P. Caucal, FS, and R. Venugopalan (2021)

Collinear non-slow divergences

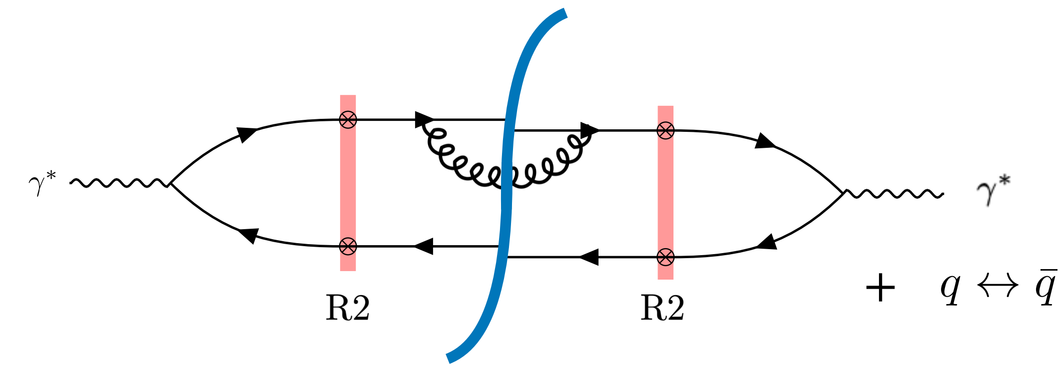

- Implement a jet algorithm* (small cone) <u>excluding slow gluon divergence</u>

Phase space for collinear non-slow gluon

$$\int_{z_f}^{z_j} \frac{\mathrm{d}z_g}{z_g} \mu^{\varepsilon} \int \frac{\mathrm{d}^{2-\varepsilon}\mathcal{C}_{qg,\perp}}{(2\pi)^{2-\varepsilon}} \frac{1}{\mathcal{C}_{qg,\perp}^2}$$

Small-cone condition:

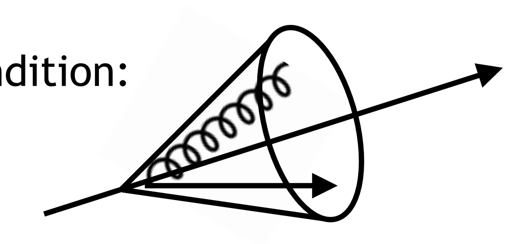

$$\mathcal{C}_{qg,\perp}^2 \leq \mathcal{C}_{qg,\perp}^2\big|_{\max} = R^2 \boldsymbol{p}_j^2 \min\left(\frac{z_g^2}{z_j^2}, \frac{(z_j - z_g)^2}{z_j^2}\right)$$

- Collinear divergence cancels against IR divergence left in virtual contributions

Soft divergence

- Remaining soft divergence cancel between vertex correction after SW, and cross term real gluon emission after SW

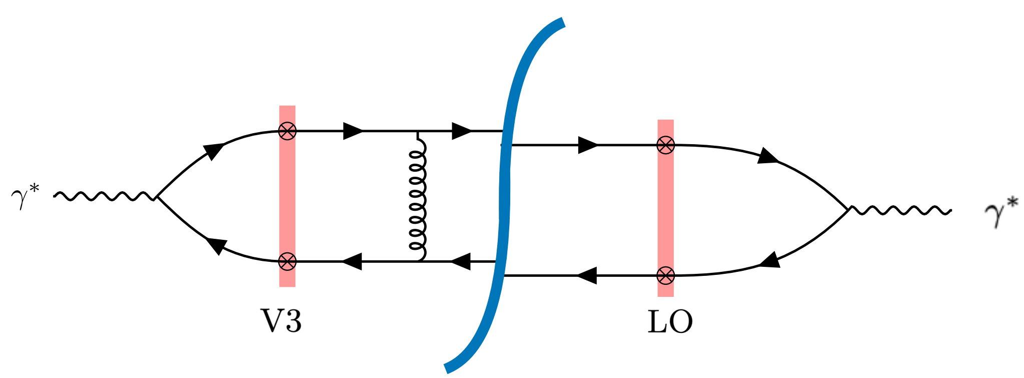

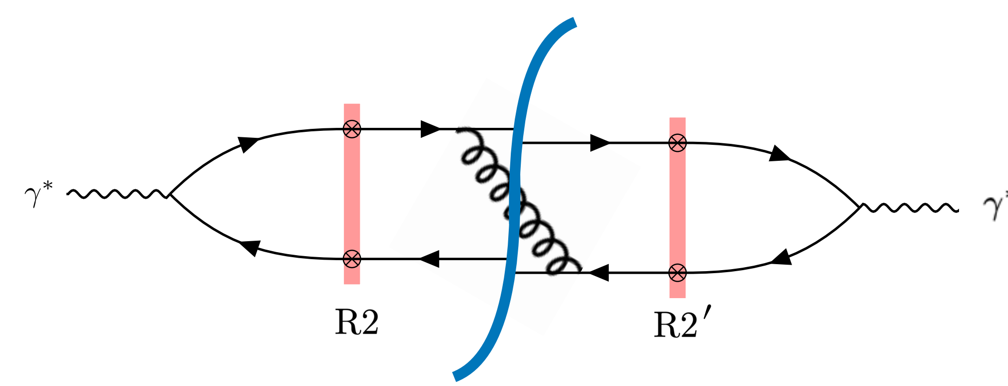

Summary

- Dijet and dihadron production in the TMD formalism

  The Weizsäcker-Williams distribution:
  gluon saturation, and linearly polarized gluons

- Dijet production beyond TMDs: CGC formalism

  From Wilson Lines to TMDs and beyond:
  Kinematic and genuine saturation corrections at the EIC

- Dijet production in the CGC at NLO

  IRC safe, JIMWLK r*apidity factorization, and*
  isolate finite impact factor.

Outlook

- Couple our partonic cross-sections to event generators

  How much of the kinematic power and genuine saturation corrections survives in the actual observable?

- Investigate dijet production at NLO in the back-to-back limit

  Recover TMD factorization   Xiao, Yuan, Zhou (2017)

  Is the ITMD framework valid at NLO?

  Isolate NLO impact factor

- Numerical implementation of dijet production at NLO

  Promoting saturation physics to a precision science

- Dijet production in DIS at two loops??